Hindawi Publishing Corporation
International Journal of Photoenergy
Volume 2012, Article ID 173865, 7 pages
doi:10.1155/2012/173865

Research Article

Highly Selective Deethylation of Rhodamine B on TiO_2 Prepared in Supercritical Fluids

Yuzun Fan,[1] Guoping Chen,[1] Dongmei Li,[1] Yanhong Luo,[1] Nina Lock,[2] Anca Paduraru Jensen,[3] Aref Mamakhel,[3] Jianli Mi,[2] Steen B. Iversen,[3] Qingbo Meng,[1] and Bo B. Iversen[2]

[1] *Beijing National Laboratory for Condensed Matter Physics, Institute of Physics, Chinese Academy of Sciences, Beijing 100190, China*
[2] *Center for Materials Crystallography, Department of Chemistry and Interdisciplinary Nanoscience Center, Aarhus University, 8000 Aarhus, Denmark*
[3] *SCF Technologies A/S, Smedeholm 13B, 2730 Herlev, Denmark*

Correspondence should be addressed to Qingbo Meng, qbmeng@iphy.ac.cn and Bo B. Iversen, bo@chem.au.dk

Received 15 June 2011; Accepted 1 July 2011

Academic Editor: Jiaguo Yu

Pure phase anatase TiO_2 nanoparticles with sizes of 5–8 nm and varying crystallinity were synthesized in supercritical isopropanol/water using a continuous flow reactor. Their photodegradation of rhodamine B (RhB) was evaluated under visible light irradiation. The as-prepared TiO_2 nanoparticles show much higher photodegradation efficiencies than commercial Degussa P25 TiO_2. Moreover, the photodegradation of RhB on the as-prepared TiO_2 follows a different process from that on P25 TiO_2, quicker N-deethylation and slower cleavage of conjugated chromophore structure. Based on PXRD, TEM, and BET measurements, these two photodegradation properties have been explained by the physicochemical properties of TiO_2.

1. Introduction

Titanium dioxide (TiO_2) has been extensively studied for degrading organic pollutants due to its high photocatalytic activity, chemical inertness, non-photocorrosion, nontoxicity, and low cost [1–7]. However, it only responds to ultraviolet light which accounts for about 4% of the solar spectrum. Photosensitization of TiO_2 by dyes has been used to utilize the visible light efficiently [8, 9]. The dye molecules absorb photons to be excited from ground state to excited state. Then the electrons are injected into the conduction band of TiO_2 while the dye molecules turn into its cationic radical. The electrons are scavenged by the molecular oxygen absorbed on the surface of TiO_2 to yield a series of active oxygen species which degrade the dye. Choosing proper organic pollutants to photosensitize TiO_2, two objectives can be achieved: (1) utilization of TiO_2 under visible light irradiation and (2) degradation of organic pollutants.

It is well known that photocatalytic reactions usually take place on the surface of the catalyst, hence the surface properties of TiO_2 are important in determining the photocatalytic activity. These properties include morphology [10, 11], particle size [12], crystal structure [13–15], crystallinity [16], pH value of the particle suspension [3], and adsorption of potential pollutants [17, 18]. Tuning the surface properties of TiO_2 photocatalysts through the preparation method is a primary way to enhance its activity [19, 20]. Recently, supercritical fluids have been used as reaction media for synthesis of nanomaterials [21–25]. Supercritical fluids exhibit physicochemical properties which are between those of liquids and gasses. Furthermore, the solubility can be effectively manipulated by small continuous changes in pressure and temperature around the critical point. The use of supercritical fluids as solvents gives significantly lower particle sizes in the nanometer range. This is believed to be due to the fact that instantaneous crystal nucleation and crystallization are faster than crystal growth. Furthermore, the method is fast and environmentally friendly, as the precursors are typically solutions of simple metal salts in water or alcohols. The short synthesis time enables synthesis under

continuous flow as an alternative to conventional batch reactions giving less operational downtime. The supercritical fluid technique may be a new way for preparation of highly active photocatalysts.

Most supercritical fluid studies of TiO_2 nanoparticles have focused on their physical characterization [21–23]. In this paper, we have synthesized nanocrystalline anatase TiO_2 in supercritical isopropanol/water. Attention was focused on evaluating their photodegradation of rhodamine B (RhB) under visible light irradiation. The results indicate that the photodegradation efficiencies of our synthesized TiO_2 are significantly higher than that of the standard photocatalyst P25 TiO_2. The photodegradation pathways for RhB, namely, cleavage of the conjugated chromophore structure and N-deethylation, were also investigated.

2. Experimental

2.1. Supercritical Synthesis of TiO_2. Degussa P25 TiO_2, which is a mixture of anatase and rutile in the weight ratio 8 : 2, was used as purchased. A series of TiO_2 samples, herein referred to as the 102 series, was prepared in a continuous flow supercritical process similar to that described in [22], but with a proprietary mixing zone design, that promotes an extremely fast and efficient mixing. The TiO_2 samples were synthesized using a first fluid with a flow rate of 24 mL/min of 0.25 M Titanium TetraIsoPropoxide (TTIP) in isopropanol and a second fluid (48 mL/min flow rate) comprising water adjusted to pH 11.2 using NH_4OH. The two fluid streams were pressurized to 300 bars. The reaction temperature in the mixing zone was controlled by heating fluid number two to the temperature required to obtain a specific temperature in the mixing zone. Fluid one was in all cases preheated to 100°C. The reactions were quenched immediately after the mixing zone. The TiO_2 samples 102-1 and 102-2 were synthesized in a two step procedure. First, a particle suspension was produced at one temperature, and subsequently this particle suspension was recirculated to the mixing zone as fluid and heated to a second temperature by mixing with fluid two in the same flow ratio. Thus, the TiO_2 samples 102-1 and 102-2 were first synthesized at 180°C and 280°C, respectively, in the mixing zone and recirculated through the system at 320°C. Sample 102-3 was synthesized directly at a mixing zone temperature of 270°C without recirculation. The residence time in the mixing chamber was from 12 s at 180°C to 9.5 s at 320°C. The residence time decreases with increasing the temperature due to the density decrease with increasing the temperature. Hence, the total reaction time is of the order 20 s for the two-step procedure (102-1, 102-2) and approximately 10 s for the directly synthesized sample 102-3. The main motivation for recirculating the nanoparticles in the reactor is to achieve a high crystallinity without substantially decreasing the surface area due to crystal growth. In the first synthesis it is expected that the particles primarily consist of a crystalline core with an amorphous shell. Upon reheating further crystallization will first take place from the outside of the particles, since this region is heated first. The produced suspensions were processed to dry powders in a rotary evaporator. The powder was redispersed to a 30 wt% suspension of particles in ethanol using a Netzsch nanomill with 60 micron ZrO_2 particles as milling media.

2.2. Characterization. Powder X-ray diffraction (PXRD) data were collected on an STOE diffractometer in transmission geometry using Cu $K\alpha_1$ radiation. Transmission electron microscopy (TEM) images were recorded on a Philips CM20 electron microscope equipped with a LaB_6 filament at 200 kV. Diffuse reflection spectra were measured on a UV-visible spectrophotometer (UV-2550, Shimadzu). The Brunauer-Emmett-Teller (BET) specific surface area was determined by nitrogen adsorption-desorption isotherm measurements at 77 K (ASAP 2020, Micromeritics).

2.3. Photodegradation Performance. The photodegradation efficiencies of the samples were determined based on the degradation of RhB under visible light irradiation. The light source was a 500 W halogen lamp (Institute of Electric Light Source, Beijing) which was fixed inside a cylindrical pyrex vessel and cooled by a circulating water jacket (pyrex). A long-pass glass filter was used to cut off the light with wavelengths below 420 nm before the sample was irradiated. The radial flux was measured with a radiant power/energy meter (70260, Oriel); the average light intensity was 100 $mW \cdot cm^{-2}$. For a typical photodegradation test, a reaction solution was prepared from 25 mg of the nanocrystalline TiO_2 sample and 50 mL of 2×10^{-5} M RhB aqueous solution. The pH value of the reaction solutions was controlled at about 5.2. The solutions were magnetically stirred in the dark for 30 minutes to ensure the establishment of an adsorption/desorption equilibrium of RhB on the TiO_2 surfaces. At certain time intervals during the irradiation, 3 mL of the turbid reaction solution was centrifuged to remove the TiO_2 catalyst. The concentration of RhB was determined by measuring the absorbance of the resulting clear solution with a UV-visible spectrophotometer (UV-2550, Shimadzu).

3. Results and Discussion

The TiO_2 samples were characterized by PXRD (Figure 1). The diffraction pattern of the 102 series samples can be indexed as the anatase phase of TiO_2, whereas additional diffraction peaks corresponding to the rutile phase of TiO_2 are observed for P25 TiO_2. The peaks of the 102 series samples are broader than those of P25 TiO_2, indicating the samples prepared in supercritical fluids consist of smaller crystallites.

The 102 series powders were mixed with CaF_2, and PXRD data were collected and Rietveld refined allowing determination of the particle size and crystallinity (i.e., determination of the fraction of crystalline material in the sample). Two parameters were used to describe the profile of each phase with a Thompson-Cox-Hastings pseudo-Voigt function. The Gaussian W parameter and the Lorentzian size parameter Y were used for the description of the TiO_2 peak shapes, while the CaF_2 peak shapes were described using

Table 1: Summary of physicochemical properties of TiO_2.

Sample[a]	Crystallite size (nm)	BET (m^2/g)	Dye adsorp. (%)	Dye degradation (%)[b]	Crystallinity (%)
102-1	7.8	239	9.3	76.9	55
102-2	7.5	229	5.4	65.0	58
102-3	5.0	346	19.7	95.8	50
P25	21	52	2.5	20.6	73(anatase)/18(rutile)

[a]The nanoparticles were used for RhB degradation with an initial dye concentration of 2×10^{-5} M and a catalyst concentration of 0.5 g/L.
[b]The dye degradation was obtained after visible irradiation for 60 min.

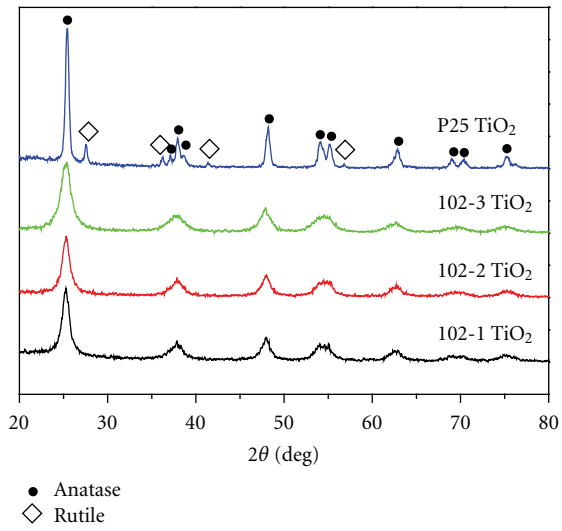

Figure 1: PXRD patterns of the TiO_2 nanoparticles.

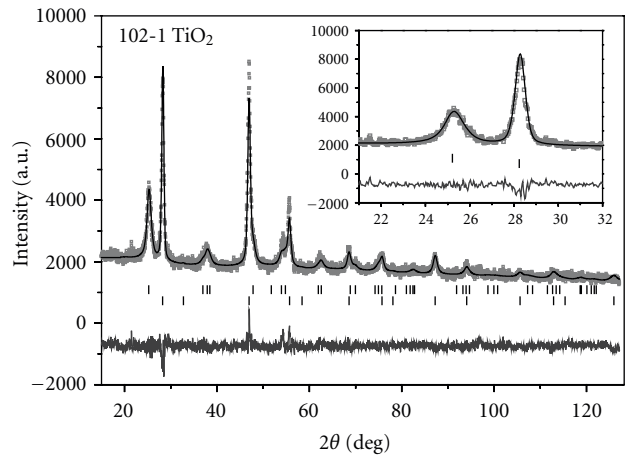

Figure 2: Rietveld refinement of a 102-1 TiO_2/CaF_2 mixture. The vertical lines indicate Bragg positions for anatase (top) and CaF_2 (bottom), respectively. The inset shows an enlargement of the angular region 21–32°, in which the peak at 25.5° is the TiO_2 (101) peak. The R_F factors are 7.0% and 6.5%, respectively, for the TiO_2 and CaF_2 phases.

W and the Lorentzian strain parameter X [24, 26]. As an example the refinement of 102-1 TiO_2/CaF_2 is shown in Figure 2. The fit of the peak at 53° is rather poor and may point to some degree of anisotropy of the particles, which is not described by this Rietveld model. However, previous TEM studies have shown that a spherical model is generally a good approach to describe nanocrystalline TiO_2 synthesized in supercritical fluids [21].

The full width at half maximum (FWHM) of the (101) TiO_2 peak was calculated from the profile parameters, and the instrumental broadening, determined from PXRD data collected on a silicon standard, was subtracted. The crystallite sizes, d, are determined from the FWHM of the (101) peak using the Scherrer equation: $d = 0.9\lambda/(\beta \cos\theta)$, where λ (0.154056 nm) is the X-ray wavelength, θ is the angle of Bragg diffraction, and β is the difference between the FWHM and the instrumental broadening. The results are shown in Table 1. The crystallite size decreases as P25 > 102-2∼102-1 > 102-3. A TEM image of the 102-3 sample is shown in Figure 3. There is a good agreement between the sizes determined from the PXRD data and TEM.

The phase fractions of crystalline TiO_2 and CaF_2 were determined by Rietveld refinement. Based on these, the crystallinity of the TiO_2 samples were determined (see Table 1).

Figure 4 presents the UV-visible diffuse reflection spectra of TiO_2. The absorption band edges of the 102 series samples

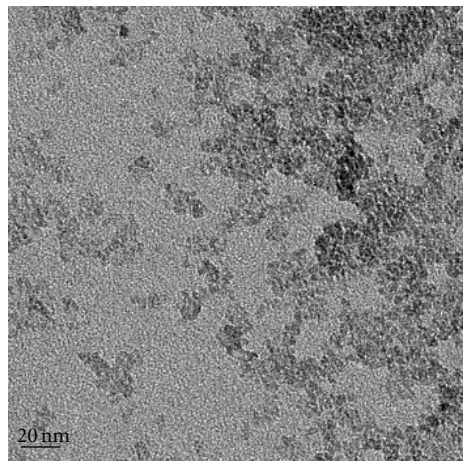

Figure 3: TEM image of the 102-3 TiO_2 sample.

of TiO_2 are blue shifted compared with that of P25 TiO_2. This can be explained by the sample composition, as anatase has a larger bandgap (3.2 eV) than rutile (3.0 eV). The 102 series of TiO_2 consists of pure anatase, while P25 TiO_2 is a mixture of anatase and rutile. For the 102 series of TiO_2, due to the quantum size effect, the order of the hypsochromic shifts of the absorption band edge is 102-3 > 102-1∼102-2.

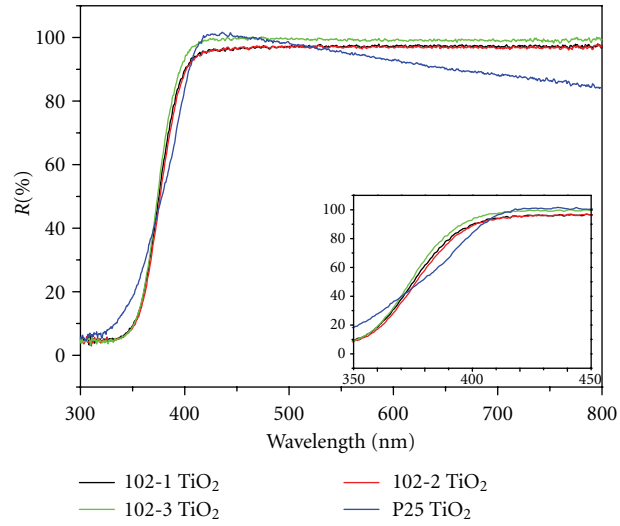

Figure 4: UV-visible diffuse reflection spectra of TiO_2. The inset shows an enlarged UV-Visible diffuse reflection spectra between 350 and 450 nm.

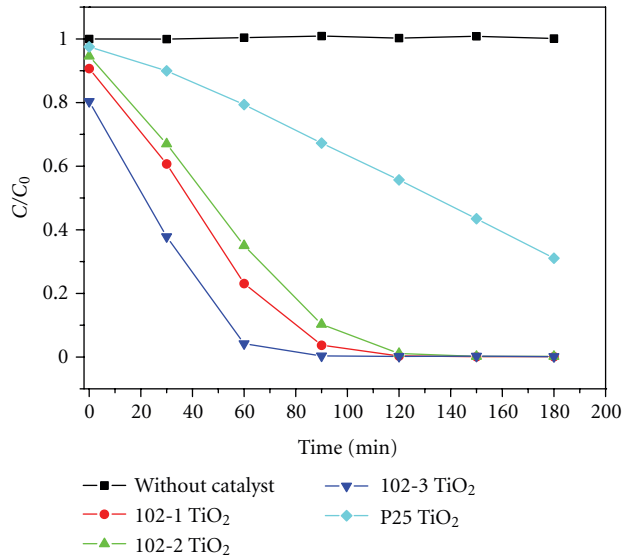

Figure 5: RhB concentration changes during the photodegradation of RhB. C_0 is the initial RhB concentration before adsorption to the TiO_2 surfaces, and C is the temporal concentration of RhB after equilibrium adsorption.

Due to the overlap between the energy distribution function of the excited RhB and the conduction band of TiO_2 [3, 27], TiO_2 can be photosensitized by RhB dye to utilize the visible light efficiently. Figure 5 shows the photodegradation of RhB by TiO_2 samples under visible light irradiation. As can be seen RhB is very stable in aqueous solution without presence of a photocatalyst. The decrease in the RhB concentration ($C/C_0 < 1$) before irradiation at $t = 0$ min reflects the extent of dye adsorbed onto the TiO_2 photocatalyst. The amounts of adsorbed dye on the 102-1, 102-2, and 102-3 TiO_2 are 9.3%, 5.4%, and 19.7%, respectively, which is much greater than that on the P25 TiO_2 (2.5%). The degradation rates of the 102 series of TiO_2 are correspondingly much greater than that of the P25 TiO_2. After visible light irradiation for 60 min, the percentage of the degraded dye for the 102-1, 102-2, 102-3, and P25 TiO_2 are 76.9%, 65.0%, 95.8%, and 20.6%, respectively. These results could be well explained by the specific surface area since the photodegradation reaction takes place on the surface of the photocatalyst. The BET surface areas of the TiO_2 samples were determined to be 239 m^2/g for 102-1 TiO_2, 229 m^2/g for 102-2 TiO_2, 346 m^2/g for 102-3 TiO_2, and 52 m^2/g for P25 TiO_2. The specific surface area of the 102 series of TiO_2 is obviously larger than that of P25 TiO_2, which is attributed to the relatively small crystallite sizes of the 102 TiO_2 samples. This accounts for the enhanced photodegradation activity of the 102 series. As summed up in Table 1 the 102 TiO_2 samples have smaller crystallite sizes, larger specific surface areas, and higher dye adsorption than P25. This leads to better photodegradation efficiencies. It is interesting to note that the data indicate that crystallite size and dye adsorption efficiency are the primary factors determining the photodegradation efficiency. Thus, the smallest nanoparticles, 102-3 (~5 nm), clearly outperform the larger 102-1 and 102-2 nanoparticles (~7-8 nm).

During the photodegradation of RhB a clear difference in the spectral change between the P25 TiO_2 and 102 series of TiO_2 is observed. Thus, there are clear differences in the extent of blue-shift in the major absorption band of RhB (Figure 6(a)). Basically, there are two photodegradation pathways for RhB: (1) cleavage of the whole conjugated chromophore structure and (2) N-deethylation [18, 28, 29]. Following the first pathway the main peak position remains constant while the peak intensity decreases. During the second pathway, which has the N-deethylation, the main peak position gradually blue shifts according to the following absorption maxima: RhB, 554 nm; N,N,N′-Triethyl-rhodamine, 539 nm; N.N′-Diethyl-rhodamine, 522 nm; N-Ethyl-rhodamine, 510 nm; Rhodamine, 498 nm [30]. In most cases the two degradation pathways coexist and compete.

For the P25 TiO_2 dispersion the major absorption band decreases gradually with little blue shift (Figure 6(b)), indicating that the cleavage of the whole conjugated chromophore structure is the main pathway. In contrast, for the 102 series of TiO_2, exemplified by 102-3 TiO_2, the major absorption band shifts from 554 to 498 nm within 90 min irradiation and upon further irradiation rhodamine undergoes a slower decomposition (Figure 6(c)), indicating N-deethylation as the main pathway. The cleavage of the conjugated chromophore structure can be estimated by the peak intensity. From the molar extinction coefficient ε_{max} (RhB, $11.5 \times 10^4\ M^{-1}\cdot cm^{-1}$; rhodamine, $8.4 \times 10^4\ M^{-1}\cdot cm^{-1}$), rhodamine should have a peak intensity at 498 nm of ca. 70% of the RhB intensity at 554 nm assuming the conjugated ring structure is not destroyed [31]. For the 102-3 TiO_2 dispersion, after full N-deethylation (90 min irradiation), about 11.7% of the conjugated chromophore structure is destroyed, and about 33% is destroyed after 180 min irradiation, which indicates initially quick N-deethylation and slow cleavage of the conjugated chromophore structure. For the P25 TiO_2 dispersion, about 68.9% is destroyed within

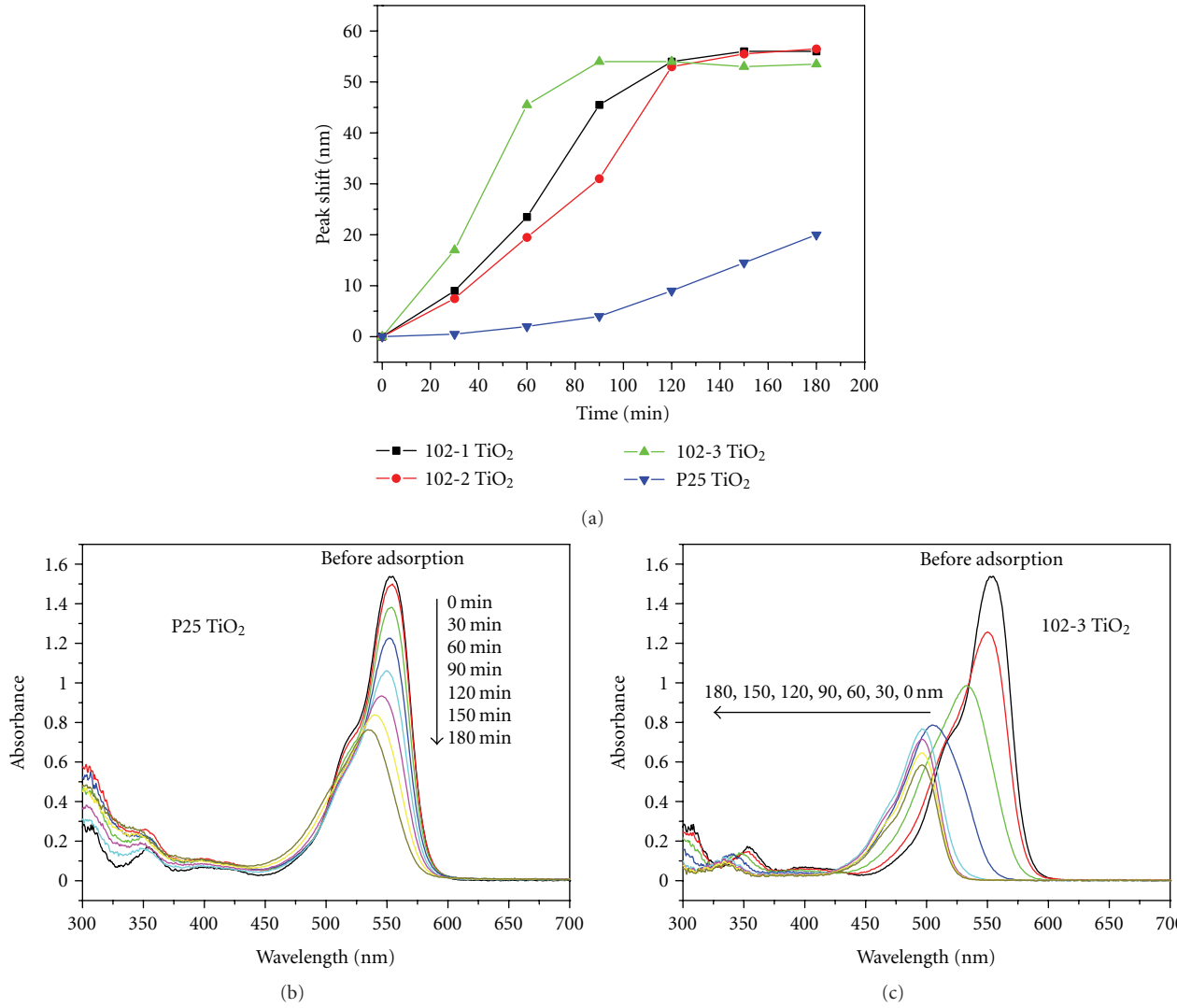

Figure 6: (a) Hypsochromic shifts of the major absorption band of RhB with irradiation time. (b) Gradual spectral changes of RhB in aqueous P25 TiO_2 dispersion under visible light irradiation. (c) Gradual spectral changes of RhB in aqueous 102-3 TiO_2 dispersion under visible light irradiation.

180 min irradiation, which means slow N-deethylation and relatively fast cleavage of conjugated chromophore structure. The difference in the degradation process of RhB between the P25 TiO_2 and 102 series of TiO_2 may be due to their different crystallinity. Lower crystallinity leads to quicker N-deethylation and slower cleavage of conjugated chromophore structure (102 series of TiO_2), while higher crystallinity leads to slower N-deethylation and quicker cleavage of conjugated chromophore structure (P25 TiO_2).

4. Conclusions

TiO_2 nanoparticles synthesized in supercritical isopropanol/water have smaller crystallite sizes, larger specific surface area, and higher dye adsorption efficiency than commercial P25 TiO_2. This leads to higher photodegradation efficiencies in degradation of rhodamine B than for P25 TiO_2. Interestingly, rhodamine B undergoes quicker N-deethylation and slower cleavage of conjugated chromophore structure on the 102 series of TiO_2 than on P25 TiO_2. The absolute crystallinity of the nanoparticles seems to affect the photodegradation process to a large extent: the lower crystallinity, the quicker N-deethylation, and slower cleavage of conjugated chromophore structure.

Acknowledgments

This work was financially supported by the National Natural Science Foundation of China (Grant no. 20725311, 20873178, 21073231, and 51072221), the Ministry of Science and Technology of China (863 Project, no. 2009AA033101), Foundation of the Chinese Academy of Sciences (no. KJCX2-YW-W27, KGCX2-YW-386-1, KGCX2-YW-363), and the Danish Strategic Research Council and the Danish National Research Foundation.

References

[1] A. Fujishima, X. Zhang, and D. A. Tryk, "TiO_2 photocatalysis and related surface phenomena," *Surface Science Reports*, vol. 63, no. 12, pp. 515–582, 2008.

[2] M. R. Hoffmann, S. T. Martin, W. Choi, and D. W. Bahnemann, "Environmental applications of semiconductor photocatalysis," *Chemical Reviews*, vol. 95, no. 1, pp. 69–96, 1995.

[3] C. Chen, W. Ma, and J. Zhao, "Semiconductor-mediated photodegradation of pollutants under visible-light irradiation," *Chemical Society Reviews*, vol. 39, no. 11, pp. 4206–4219, 2010.

[4] J.-M. Herrmann, "Heterogeneous photocatalysis: state of the art and present applications," *Topics in Catalysis*, vol. 34, no. 1-4, pp. 49–65, 2005.

[5] F. Han, V. S. R. Kambala, M. Srinivasan, D. Rajarathnam, and R. Naidu, "Tailored titanium dioxide photocatalysts for the degradation of organic dyes in wastewater treatment: a review," *Applied Catalysis A*, vol. 359, no. 1-2, pp. 25–40, 2009.

[6] J. A. Byrne, P. A. Fernandez-Ibañez, P. S. M. Dunlop, D. M. A. Alrousan, and J. W. J. Hamilton, "Photocatalytic enhancement for solar disinfection of water: a review," *International Journal of Photoenergy*, vol. 2011, Article ID 798051, 12 pages, 2011.

[7] J. Gamage and Z. S. Zhang, "Applications of photocatalytic disinfection," *International Journal of Photoenergy*, vol. 2010, Article ID 764870, 11 pages, 2010.

[8] J. Zhao, T. Wu, K. Wu, K. Oikawa, H. Hidaka, and N. Serpone, "Photoassisted degradation of dye pollutants. 3. Degradation of the cationic dye rhodamine B in aqueous anionic surfactant/TiO_2 dispersions under visible light irradiation: evidence for the need of substrate adsorption on TiO_2 particles," *Environmental Science and Technology*, vol. 32, no. 16, pp. 2394–2400, 1998.

[9] B. O'Regan and M. Grätzel, "A low-cost, high-efficiency solar cell based on dye-sensitized colloidal TiO_2 films," *Nature*, vol. 353, no. 6346, pp. 737–740, 1991.

[10] N. H. Lee, H. J. Oh, S. C. Jung, W. J. Lee, D. H. Kim, and S. J. Kim, "Photocatalytic properties of nanotubular-shaped TiO_2 powders with anatase phase obtained from titanate nanotube powder through various thermal treatments," *International Journal of Photoenergy*, vol. 2011, Article ID 327821, 7 pages, 2011.

[11] M. L. Chen and W. C. Oh, "The improved photocatalytic properties of methylene blue for V_2O_3/CNT/TiO_2 composite under visible light," *International Journal of Photoenergy*, vol. 2010, Article ID 264831, 5 pages, 2010.

[12] H. D. Jang, S. K. Kim, and S. J. Kim, "Effect of particle size and phase composition of titanium dioxide nanoparticles on the photocatalytic properties," *Journal of Nanoparticle Research*, vol. 3, no. 2-3, pp. 141–147, 2001.

[13] J. Zhang, Q. Xu, Z. Feng, M. Li, and C. Li, "Importance of the relationship between surface phases and photocatalytic activity of TiO_2," *Angewandte Chemie International Edition*, vol. 47, no. 9, pp. 1766–1769, 2008.

[14] Y. Wang, L. Zhang, K. Deng, X. Chen, and Z. Zou, "Low temperature synthesis and photocatalytic activity of rutile TiO_2 nanorod superstructutes," *Journal of Physical Chemistry C*, vol. 111, no. 6, pp. 2709–2714, 2007.

[15] Z. Ding, G. Q. Lu, and P. F. Greenfield, "Role of the crystallite phase of TiO_2 in heterogeneous photocatalysis for phenol oxidation in water," *Journal of Physical Chemistry B*, vol. 104, no. 19, pp. 4815–4820, 2000.

[16] M. E. Simonsen, H. Jensen, Z. Li, and E. G. Søgaard, "Surface properties and photocatalytic activity of nanocrystalline titania films," *Journal of Photochemistry and Photobiology A*, vol. 200, no. 2-3, pp. 192–200, 2008.

[17] F. Chen, J. Zhao, and H. Hidaka, "Highly selective deethylation of Rhodamine B: adsorption and photooxidation pathways of the dye on the TiO_2/SiO_2 composite photocatalyst," *International Journal of Photoenergy*, vol. 5, no. 4, pp. 209–217, 2003.

[18] Q. Wang, C. Chen, D. Zhao, W. Ma, and J. Zhao, "Change of adsorption modes of dyes on fluorinated TiO_2 and its effect on photocatalytic degradation of dyes under visible irradiation," *Langmuir*, vol. 24, no. 14, pp. 7338–7345, 2008.

[19] Q. J. Xiang, J. G. Yu, and M. Jaroniec, "Tunable photocatalytic selectivity of TiO_2 films consisted of flower-like microspheres with exposed 001 facets," *Chemical Communications*, vol. 47, no. 15, pp. 4532–4534, 2011.

[20] S. Liu, J. Yu, and M. Jaroniec, "Tunable photocatalytic selectivity of hollow TiO_2 microspheres composed of anatase polyhedra with exposed 001 facets," *Journal of the American Chemical Society*, vol. 132, no. 34, pp. 11914–11916, 2010.

[21] P. Hald, J. Becker, M. Bremholm et al., "Supercritical propanol-water synthesis and comprehensive size characterisation of highly crystalline anatase TiO_2 nanoparticles," *Journal of Solid State Chemistry*, vol. 179, no. 8, pp. 2674–2680, 2006.

[22] L. L. Toft, D. F. Aarup, M. Bremholm, P. Hald, and B. B. Iversen, "Comparison of T-piece and concentric mixing systems for continuous flow synthesis of anatase nanoparticles in supercritical isopropanol/water," *Journal of Solid State Chemistry*, vol. 182, no. 3, pp. 491–495, 2009.

[23] H. Jensen, K. D. Joensen, S. B. Iversen, and E. G. Søgaard, "Low temperature synthesis of metal oxides by a supercritical seed enhanced crystallization (SSEC) process," *Industrial and Engineering Chemistry Research*, vol. 45, no. 10, pp. 3348–3353, 2006.

[24] N. Lock, P. Hald, M. Christensen, H. Birkedal, and B. B. Iversen, "Continuous flow supercritical water synthesis and crystallographic characterization of anisotropic boehmite nanoparticles," *Journal of Applied Crystallography*, vol. 43, no. 4, pp. 858–866, 2010.

[25] J. Becker, P. Hald, M. Bremholm et al., "Critical size of crystalline ZrO_2 nanoparticles synthesized in near- and supercritical water and supercritical isopropyl alcohol," *ACS Nano*, vol. 2, no. 5, pp. 1058–1068, 2008.

[26] H. Jensen, K. D. Joensen, J. E. Jørgensen, J. S. Pedersen, and E. G. Søgaard, "Characterization of nanosized partly crystalline photocatalysts," *Journal of Nanoparticle Research*, vol. 6, no. 5, pp. 519–526, 2004.

[27] T. Takizawa, T. Watanabe, and K. Honda, "Photocatalysis through excitation of adsorbates. 2. A comparative study of rhodamine B and methylene blue on cadmium sulfide," *Journal of Physical Chemistry*, vol. 82, no. 12, pp. 1391–1396, 1978.

[28] H. Park and W. Choi, "Photocatalytic reactivities of nafion-coated TiO_2 for the degradation of charged organic compounds under UV or visible light," *Journal of Physical Chemistry B*, vol. 109, no. 23, pp. 11667–11674, 2005.

[29] K. Yu, S. Yang, H. He, C. Sun, C. Gu, and Y. Ju, "Visible light-driven photocatalytic degradation of rhodamine B over $NaBiO_3$: pathways and mechanism," *Journal of Physical Chemistry A*, vol. 113, no. 37, pp. 10024–10032, 2009.

[30] T. Watanabe, T. Takizawa, and K. Honda, "Photocatalysis through excitation of adsorbates. 1. Highly efficient

N-deethylation of rhodamine B adsorbed to CdS," *Journal of Physical Chemistry*, vol. 81, no. 19, pp. 1845–1851, 1977.

[31] T. Wu, G. Liu, J. Zhao, H. Hidaka, and N. Serpone, "Photoassisted degradation of dye pollutants. V. Self-photosensitized oxidative transformation of Rhodamine B under visible light irradiation in aqueous TiO_2 dispersions," *Journal of Physical Chemistry B*, vol. 102, no. 30, pp. 5845–5851, 1998.